Supporting Information

Multi-tunable thermoresponsive behaviors of poly(amido thioether)s

Lu Lian, Qingqing Wang, Fujin Duan and Youliang Zhao*

Suzhou Key Laboratory of Macromolecular Design and Precision Synthesis, Key Laboratory of Polymeric Materials Design and Synthesis for Biomedical Function, Jiangsu Key Laboratory of Advanced Functional Polymer Design and Application, State and Local Joint Engineering Laboratory for Novel Functional Polymeric Materials, College of Chemistry, Chemical Engineering and Materials Science, Soochow University, Suzhou 215123, China. E-mail: ylzhao@suda.edu.cn.

Experimental

Materials

The chemicals were purchased from Sinopharm Chemical Reagent Co., Ltd unless otherwise stated. Acryloyl chloride (99%, Aladdin), D,L-homocysteine thiolactone hydrochloride (98%, Aladdin), *N,N*-diethylethylenediamine (DEDA, 99%), glycinamide (GAM, 99%, Aladdin), *N*-(3-aminopropyl)imidazole (API, 99%), ethanolamine (EA, 99%), 3-amino-1-propanol (APA, 99%) and other reagents with analytical grade were used as received, and *N*,*N*-dimethylformamide (DMF) was dried over CaH_2 and distilled under reduced pressure. For buffer solutions with a fixed concentration of 0.05 mol L^{-1}, the solutions with pH 3.0 and 4.0 were composed of glycine and HCl, the solutions with pH 5.0-8.0 comprised Na_2HPO_4 and KH_2PO_4 with distinct ratios, and the solutions with pH 9.0 and 10 were composed of glycine and NaOH. *N*-Acryloylhomocysteine thiolactone (ATL) was synthesized and purified according to literature procedure.[1] Poly(*N*-(3-imidazol-1-yl-propyl)acrylamide) (PIPAA) was synthesized by free radical polymerization of IPAA using AIBN as an initiator ($[IPAA]_0:[AIBN]_0 = 50$, $[M]_0 = 2.0$ mol L^{-1}, in DMF at 70 °C for 20 h).[2]

Synthesis of poly(amido thioether)s

In a typical run, ATL (0.342 g, 2.0 mmol) was dissolved in DMF (3.4 mL), and the solution was bubbled with nitrogen for 15 min, followed by addition of glycinamide (0.148 g, 2.0 mmol) under nitrogen atmosphere. After stirring at 25 °C overnight, the mixture was further reacted at 90 °C for 24 h. The polymerization solution was cooled down and precipitated into cold diethyl ether. After vacuum drying, 0.328 g (67% yield) of poly(amido thioether) bearing *N*-carbamoylmethylamido side groups (abbreviated as P1) was obtained. Other poly(amido thioether)s P2-P5 were synthesized by polymerization of ATL with other primary amines (API for synthesis of P2), DEDA (for synthesis of P3), EA (for synthesis of P4) and APA (for synthesis of P5) according to similar procedures, in which the concentration of ATL was fixed at 0.10 g mL^{-1}.

P1: $M_{n,GPC}$ = 5470 Da, $Đ$ = 1.64. ^{1}H NMR (DMSO-d_6, ppm): δ 7.8-8.6 (m, CONH), 6.7-7.6 (m, CONH_2), 5.5-6.4 (m, remaining terminal CH_2=CH originating from ATL), 4.29 (m, CHNH), 3.62 (m, CONHCH_2CONH$_2$), 2.67 (m, SCH_2CH$_2$CONH), 2.2-2.6 (m, NHCOCH_2 and CONHCHCH$_2$CH_2S), 1.6-2.1 (m, CONHCHCH_2). FT-IR (KBr): 3420, 3276, 3195, 3061, 2976, 2933, 1640, 1533, 1476, 1438, 1391, 1250, 1175, 1101, 1032, 850, 804 cm^{-1}.

Poly(amido thioether) bearing *N*-(3-(1-imidazolyl)propyl)amido side groups (P2): 64% yield, $M_{n,GPC}$ = 5980 Da, $Đ$ = 1.67. ^{1}H NMR (DMSO-d_6, ppm): δ 7.8-8.5 (m, CONH), 7.61 (s, CH=N of imidazolyl group), 7.16 and 6.88 (each s, CH=CHN of imidazolyl group), 5.5-6.4 (m, remaining terminal CH_2=CH originating from ATL), 4.28 (m, CHNH), 3.93 (m, CH_2N), 3.01 (m, CONHCH_2), 2.67 (m, SCH_2CH$_2$CONH), 2.2-2.6 (m, CH_2CONHCHCH$_2$CH_2S), 1.81 (m, CONHCHCH_2CH$_2$S and CONHCH$_2$CH_2CH$_2$N). FT-IR (KBr): 3480, 3276, 3107, 3055, 2928, 1638, 1537, 1515, 1438, 1383, 1277, 1233, 1084, 1030, 914, 819, 737 cm^{-1}.

Poly(amido thioether) bearing *N*-(2-diethylaminoethyl)amido side groups (P3): 70% yield, $M_{n,GPC}$ = 4930 Da, $Đ$ = 1.69. ^{1}H NMR (DMSO-d_6, ppm): δ7.5-8.4 (m, CONH), 5.5-6.4 (m, remaining terminal CH_2=CH originating from ATL), 4.29 (m, CHNH), 3.09 (m, CONHCH_2), 2.66 (m, SCH_2CH$_2$CONH), 2.2-2.6 (m, CH_2CONHCHCH$_2$CH_2S and CH_2N), 1.6-2.0 (m, CONHCHCH_2), 0.93 (t, *J* 6.9, N(CH$_2$CH_3)$_2$). FT-IR (KBr): 3280, 3077, 2967, 2928, 2875, 2802, 1633, 1540, 1440, 1380, 1281, 1244, 1202, 1179, 1140, 1067, 985, 940, 771, 711, 680 cm^{-1}.

Poly(amido thioether) bearing *N*-(2-hydroxyethyl)amido side groups (P4): 54% yield, $M_{n,GPC}$ = 6040 Da, $Đ$ = 1.77. ^{1}H NMR (DMSO-d_6, ppm): δ 7.5-8.7 (m, CONH), 5.5-6.4 (m, remaining terminal CH_2=CH originating from ATL), 4.65 (s, CH$_2$OH), 4.32 (m, CHNH), 3.39 (m, CONHCH$_2$CH_2OH), 3.13 (m, CONHCH_2), 2.66 (m, SCH_2CH$_2$CONH), 2.2-2.6 (m, CH_2CONHCHCH$_2$CH_2S), 1.6-2.0 (m, CONHCHCH_2). FT-IR (KBr): 3275, 3078, 2925, 2878, 1628, 1530, 1431, 1387, 1362, 1246, 1205, 1053, 1017, 909, 851, 795, 769, 668 cm^{-1}.

Poly(amido thioether) bearing *N*-(3-hydroxypropyl)amido side groups (P5): 58% yield, $M_{n,GPC}$ = 6600 Da, $Đ$ = 1.93. ^{1}H NMR (DMSO-d_6, ppm): δ7.6-8.5 (m, CONH), 5.5-6.4 (m, remaining terminal CH_2=CH originating from ATL), 4.44 (m, CH$_2$OH), 4.28 (m, CHNH), 3.40 (m, CONHCH$_2$CH_2OH), 3.10 (m, CONHCH_2), 2.66 (m, SCH_2CH$_2$CONH), 2.2-2.6 (m, CH_2CONHCHCH$_2$CH_2S), 1.6-2.0 (m, CONHCHCH_2), 1.54 (m, CONHCH$_2$CH_2CH$_2$OH). FT-IR (KBr): 3276, 3075, 2925, 2874, 1628, 1532, 1434, 1379, 1309, 1248, 1199, 1148, 1053, 998, 962, 862, 769, 718, 661 cm^{-1}.

Selective oxidation of P1 and P2

In a typical run, P1 (20 mg, with 0.08 mmol of thioether group) was added to a glass tube, followed by addition of excess H_2O_2 (3% aqueous solution, 0.185 g, 0.16 mmol) and deionized water to reach a total volume of 10 mL. The reaction was conducted at 25 ^{o}C for predetermined times (t = 30, 60, 90, 120 min), and about 1.2 mL of polymer solution was drawn to perform turbidity analysis. The reaction was eventually stopped in 24 h, and the isolated polymer was denoted as P1'. Similarly, P2' was synthesized by oxidation of P2 solution (c_p = 2.0 mg mL^{-1}) using excess H_2O_2 at 25 ^{o}C for 24 h.

P1': ^{1}H NMR (DMSO-d_6, ppm): δ 7.7-8.8 (m, CONH), 6.8-7.6 (m, CONH_2), 4.0-4.6 (m, CHNH), 3.4-3.9 (m, CONHCH_2CONH$_2$ and CH_2SO$_2$CH_2), 2.9-3.3 (m, CH_2SOCH_2), 2.55-2.80 (m, NHCOCH_2), 1.70-2.45 (m, CONHCHCH_2). FT-IR (KBr): 3270, 3206, 3056, 2984, 2939, 2808, 1651, 1532, 1425, 1396, 1272, 1169, 1120, 1037, 870, 837, 803, 742 cm^{-1}.

Formation of polymer solutions

To perform TEM analysis, a solvent switch method was adopted to prepare P1 assemblies. In a typical run, P1 (10 mg) and DMF (1.0 mL) were added to a vial, followed by stirring at 25 ^{o}C for 5 h to form clear solution. Afterward, deionized water (3.0 mL) was slowly added to the polymer solution via a metering pump (with addition rate of about 1.0 mL h^{-1}) under vigorous stirring, and then the mixture was further stirred overnight to reach an equilibrium. The resultant solution was transferred into a dialysis membrane tubing (MWCO 1000), and the dialysis against deionized water was adopted to remove the organic solvent. Afterward, deionized water was carefully added to reach a total volume of 5.0 mL, followed by stirring for 2 h to form P1 assemblies with a concentration of 2.0 mg mL^{-1}. On this basis, the apparent hydrodynamic diameter (D_h) and particle size distribution (PD) of polymer assemblies were analyzed by DLS, and the morphology of nano-objects was determined by TEM.

For other measurements such as turbidity, UV-vis and fluorescence analyses, various polymers were directly dissolved or dispersed in deionized water, ethanol, water/ethanol mixture or buffer solution to prepare polymer solutions with the desired concentration.

Characterization

^{1}H NMR spectra (400 MHz) were recorded in DMSO-d_6 on a Varian Unity Inova 400 MHz spectrometer at 25 ^{o}C. Temperature-variable ^{1}H NMR spectra of polymer solutions were recorded in D_2O on an Agilent ProPulse 600 MHz spectrometer at different temperatures. Apparent molar mass ($M_{n,GPC}$) and dispersity ($Đ = M_w/M_n$) of various polymers were measured on a TOSOH HLC-8320 gel permeation chromatography (GPC) using three TSKgel SuperMultipore HZ-M columns at 40 °C, in which the pendant hydroxyl groups of P4 and P5 were converted to acetates by esterification before GPC measurement. DMF was used as the eluent at a flow rate of 0.35 mL min^{-1}, and the samples were calibrated with PMMA standard samples. Differential scanning calorimetry (DSC) was measured on Q200 DSC from TA Instruments using a heating/cooling rate of 10 K min^{-1}. Fourier Transform Infrared (FT-IR) spectra were recorded on a Bruker Vertex 70 spectrometer. UV-vis absorption spectra were recorded using a Shimadzu UV-1800 spectrophotometer. Fluorescence spectra of polymer solutions were recorded at different temperatures using a Shimadzu RF-5301 fluorescence spectrometer with an excitation wavelength of 320 nm. Turbidity analysis of polymer solutions was performed at 500 nm on a Shimadzu UV-3150 UV-vis spectrophotometer equipped with a thermoregulator, and the cloud point (LCST-type $T_{\mathrm{c,l}}$ or UCST-type $T_{\mathrm{c,u}}$) was calculated as the temperature at the half of the maximal and minimal transmittances. To determine apparent hydrodynamic diameter (D_{h}), peak hydrodynamic diameter (D_{peak}) and particle size distribution (PD) of polymer assemblies formed in aqueous solution, dynamic light scattering (DLS) analysis was performed using Zetasizer Nano-ZS from Malvern Instruments equipped with a 633 nm He-Ne laser using back-scattering detection. Transmission electron microscopy (TEM) images were measured using a Hitachi HT7700 electron microscope with an acceleration voltage of 120 kV to determine the morphology of nano-objects, in which the freeze-drying technique was used to stabilize the shape of polymer assemblies formed in aqueous solutions.

Reference

1 S. Reinicke, P. Espeel, M. M. Stamenovic and F. E. Du Prez, *ACS Macro Lett.*, 2013, **2**, 539–543.

2 Y. Lin, L. Lian, J. M. Hu, M. Zhang and Y. L. Zhao, *Macromolecules*, 2023, **56**, 5162–5172.

Table S1 Summary of chemical shifts of various protons of primary amines and their derivative side groups, in which Δδ ($\delta_{CONHCH2}$(Px) − δ_{CH2NH2}(amine)) denotes the variation of chemical shift of characteristic CH_2 during structural transformation from CH_2NH$_2$ to pendant CONHCH_2 of Px via aminolysis of thiolactone group

sample	chemical shift (ppm)	Px	chemical shift (ppm)	Δδ (ppm)
GAM	3.02 (CH_2NH$_2$)	P1	3.62 (CONHCH_2)	+0.62
API	7.60/7.15/6.87 (CH of imidazolyl), 4.00 (CH_2N), 2.46 (CH_2NH$_2$), 1.74 (CH_2CH$_2$NH$_2$)	P2	7.61/7.16/6.88 (CH of imidazolyl), 3.93 (CH_2N), 3.01 (CONHCH_2), 1.81 (CONHCH$_2$CH_2CH$_2$N)	+0.55
DEDA	2.53 (CH_2NH$_2$), 2.44/2.34 (CH_2N), 0.93 (CH_3)	P3	3.09 (CONHCH_2), 2.46/2.43 (CH_2N), 0.93 (CH_3)	+0.56
EA	3.33 (CH_2OH), 2.54 (CH_2NH$_2$)	P4	3.39 (CH_2OH), 3.13 (CONHCH_2)	+0.59
APA	3.45 (CH_2OH), 2.59 (CH_2NH$_2$), 1.48 (CH_2CH$_2$OH)	P5	3.40 (CH_2OH), 3.10 (CONHCH_2), 1.54 (CH_2CH$_2$OH)	+0.51

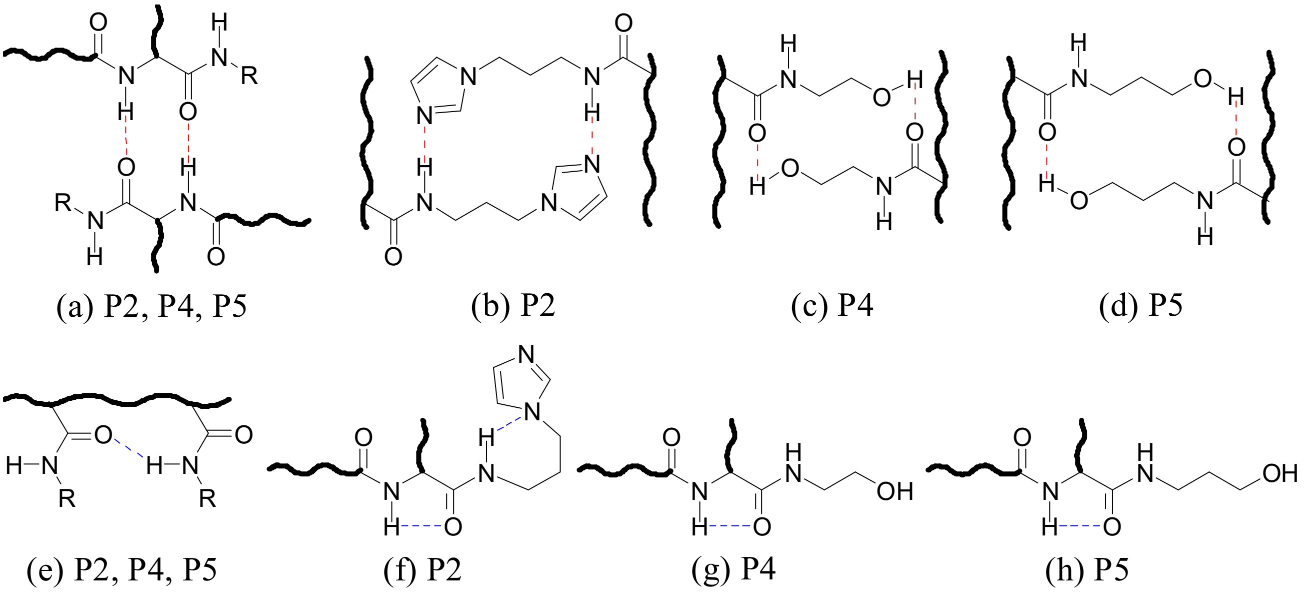

--- inter/intrachain HBs related to dual amide groups (a) and pendant groups (b-d)
--- intrachain HBs related to the neighboring (e) and same (f-h) repeating units

Scheme S1 Proposed major inter/intrachain hydrogen bonds of polymer solutions formed from P2 (a, b, e, f), P4 (a, c, e, g) and P5 (a, d, e, h) in water or PBS.

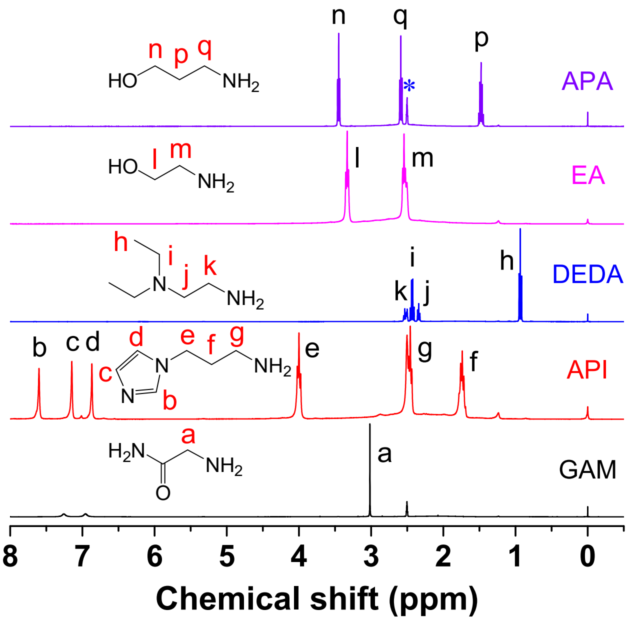

Fig. S1 ^{1}H NMR spectra of glycinamide (GAM), *N*-(3-aminopropyl)imidazole (API), *N,N*-diethylethylenediamine (DEDA), ethanolamine (EA) and 3-amino-1-propanol (APA) recorded in DMSO-d_6 (*).

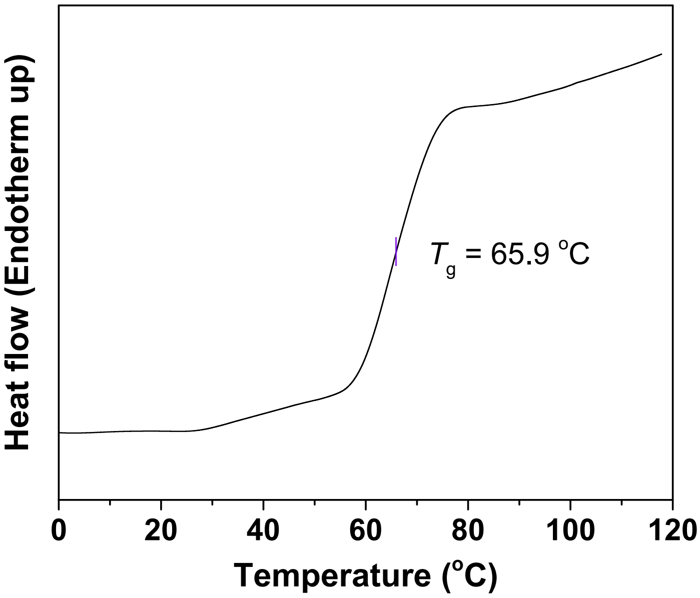

Fig. S2 DSC curve of PIPAA.

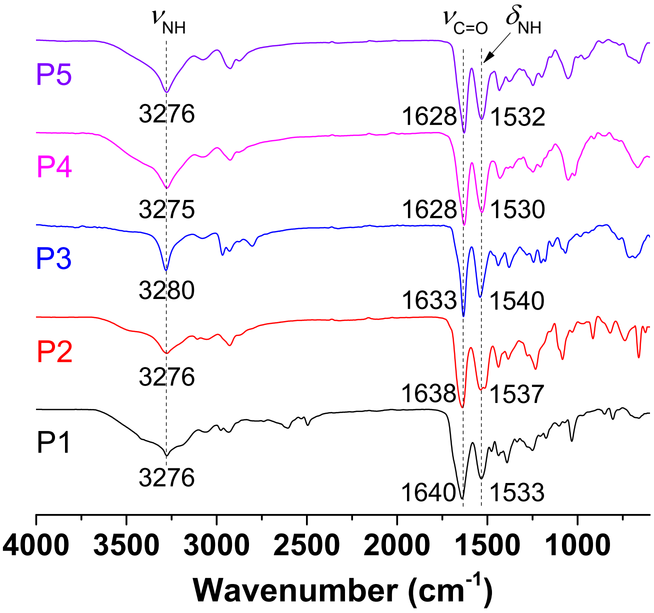

Fig. S3 FT-IR spectra of P1-P5.

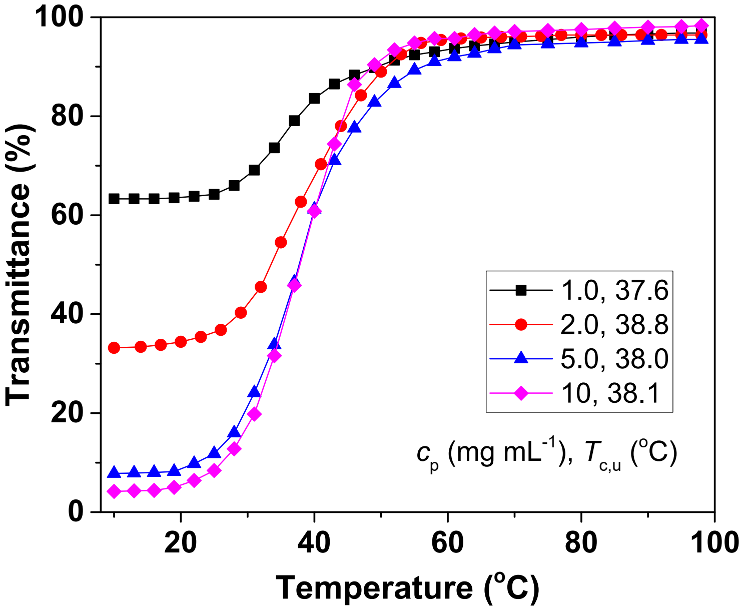

Fig. S4 Temperature-dependent transmittances of P1 aqueous solutions.

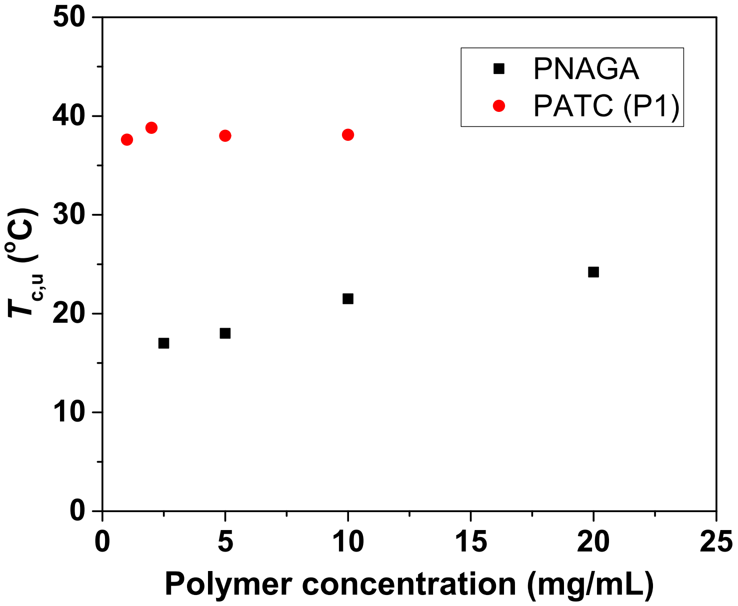

Fig. S5 Influence of polymer concentration on cloud point of PNAGA and PATC aqueous solutions, in which the results of PNAGA solutions (reference 49) are adopted for comparison.

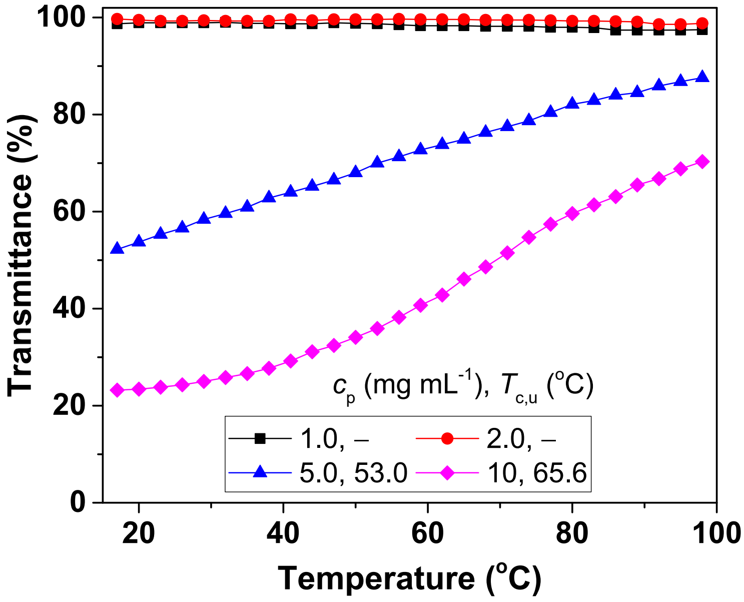

Fig. S6 Temperature-dependent transmittances of P2 aqueous solutions.

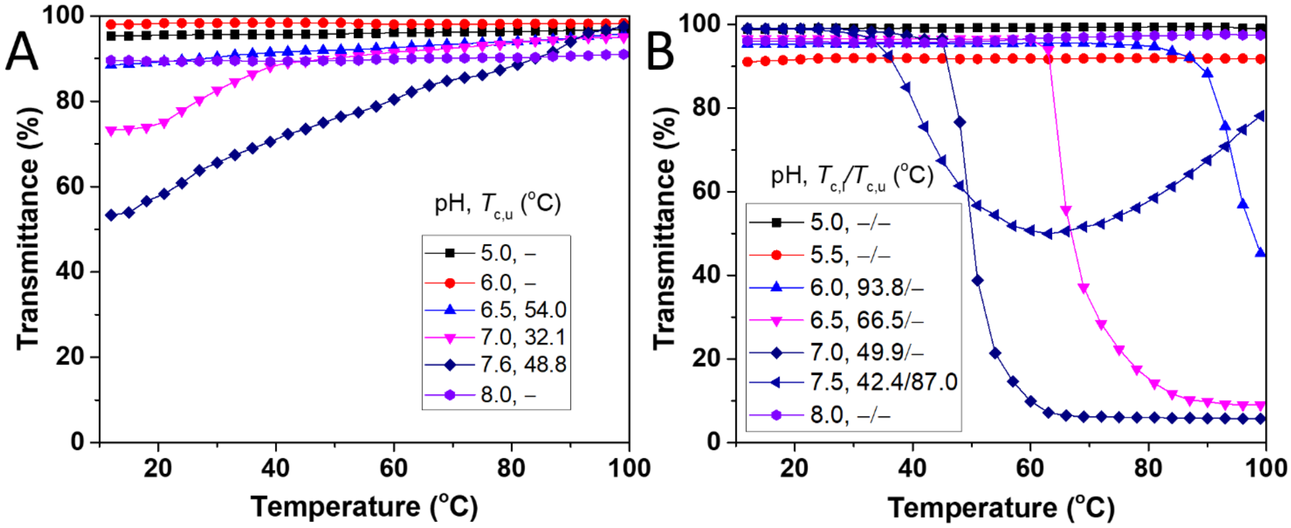

Fig. S7 Temperature-dependent transmittances of PIPAA solutions ($c_p = 2.0$ mg mL^{-1}) formed in water (A) and PBS (B) at different pH values.

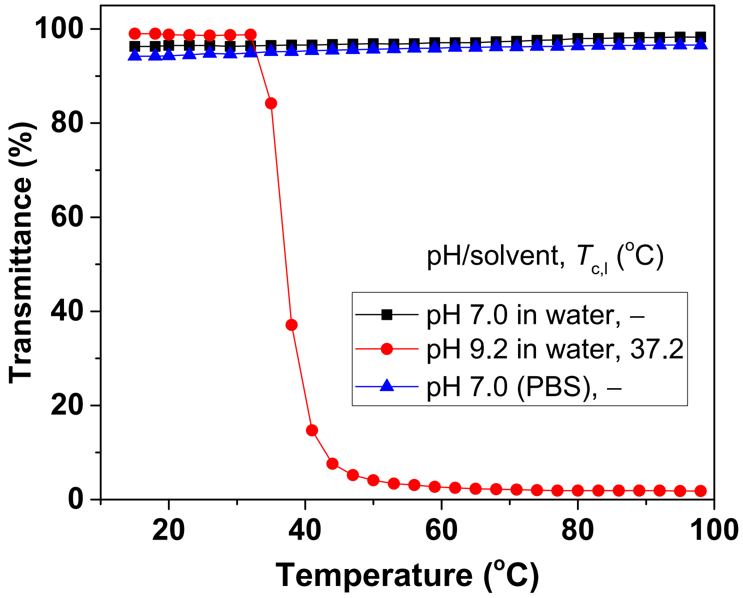

Fig. S8 Temperature-dependent transmittances of P3 solutions (c_p = 2.0 mg mL^{-1}) formed in water (pH = 7.0 or 9.2) and PBS (pH = 7.0).

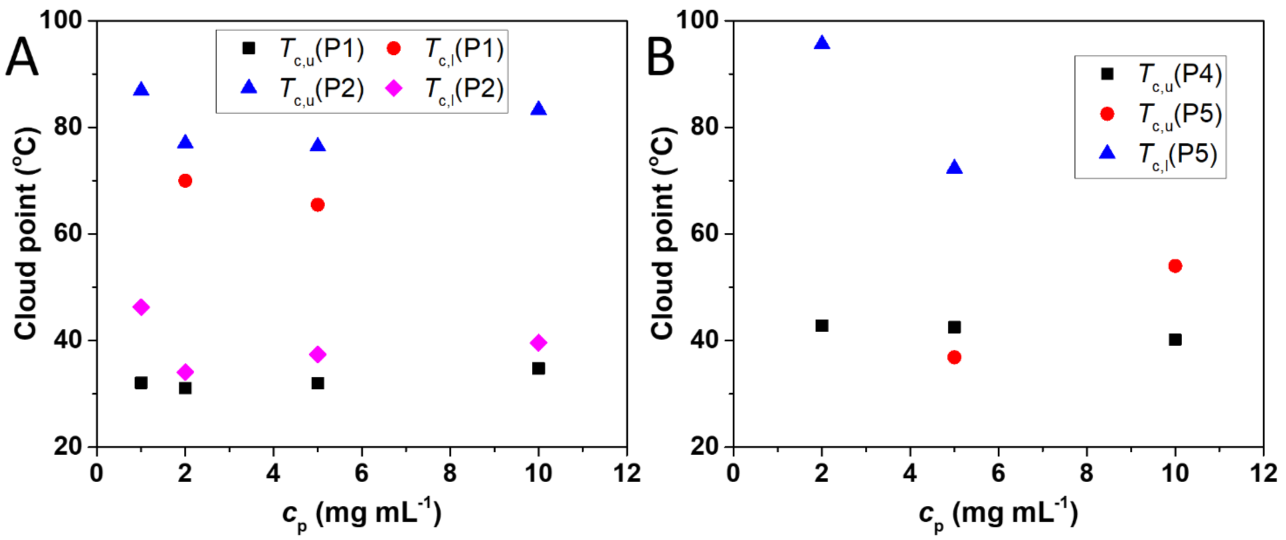

Fig. S9 Influence of polymer concentration on cloud point of polymer solutions formed from P1/P2 (A) and P4/P5 (B) in PBS (pH = 7.0).

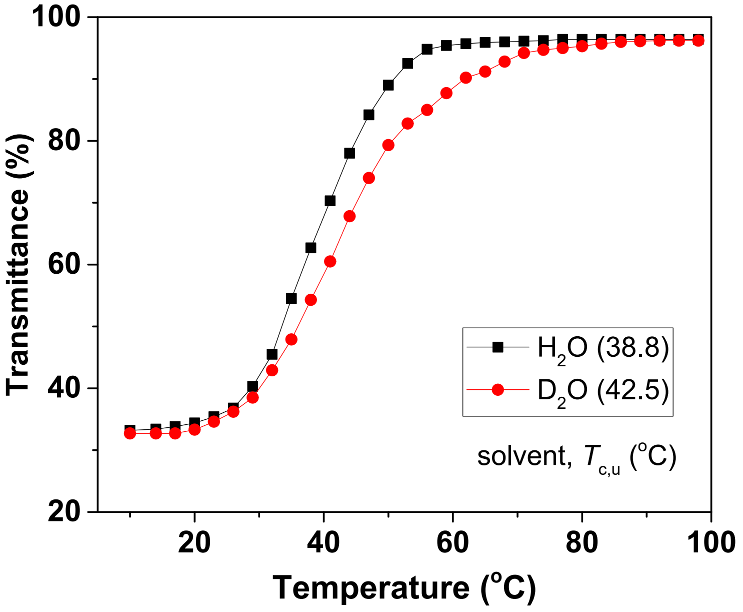

Fig. S10 Temperature-dependent transmittances of P1 solutions (c_p = 2.0 mg mL^{-1}) formed in H_2O and D_2O.

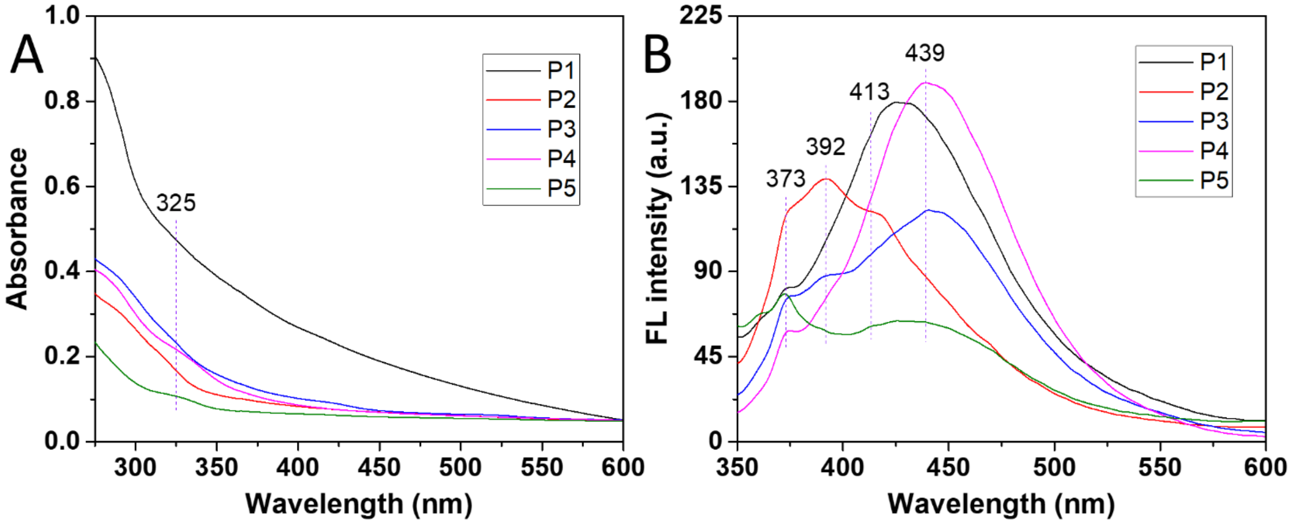

Fig. S11 UV-vis (A) and fluorescence (B, λ_{ex} = 320 nm) spectra of polymer solutions (c_p = 2.0 mg mL^{-1}) formed from P1-P5 in PBS (pH = 7.0).

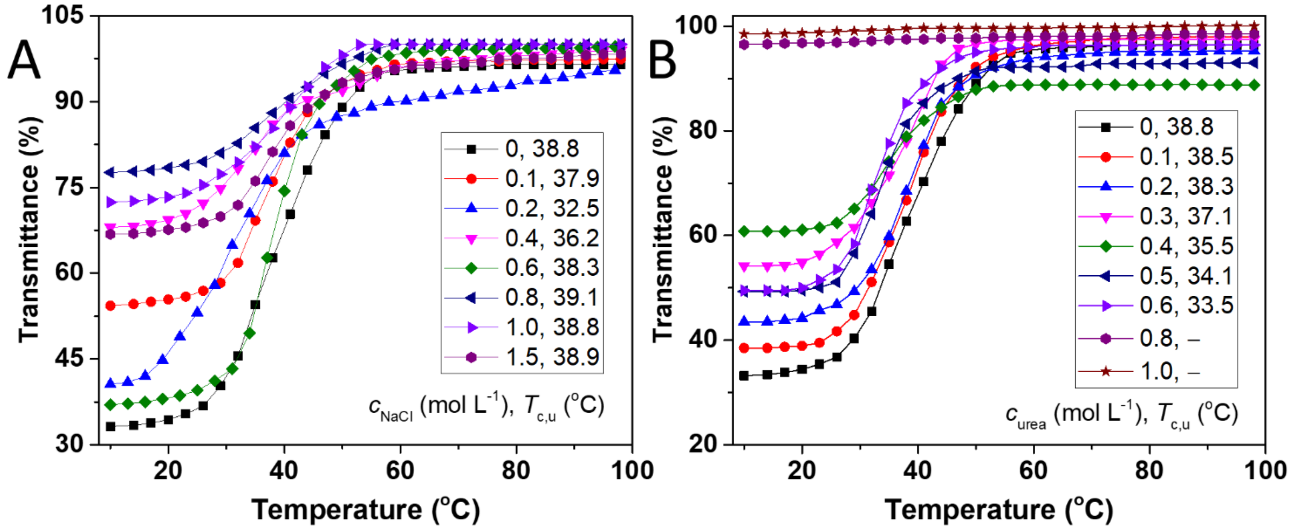

Fig. S12 Temperature-dependent transmittances of P1 aqueous solutions (c_p = 2.0 mg mL^{-1}) in the presence of NaCl (A) and urea (B) with different concentrations.

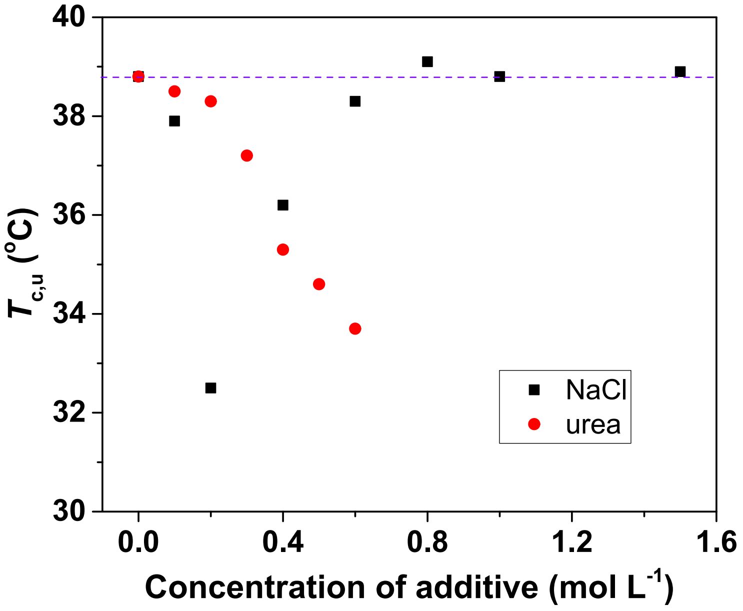

Fig. S13 Dependence of $T_{c,u}$ of P1 aqueous solutions (c_p = 2.0 mg mL^{-1}) on concentration of NaCl and urea.

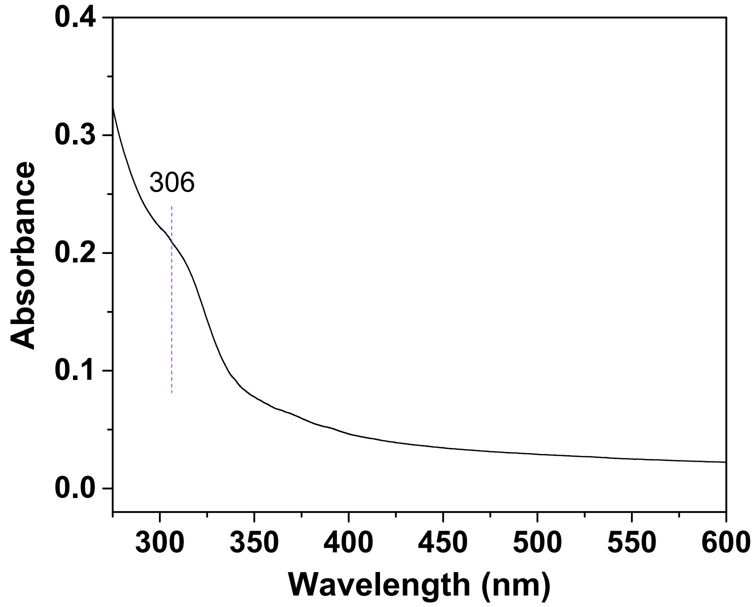

Fig. S14 UV-vis spectrum of P2 solutions (c_p = 2.0 mg mL^{-1}) formed in PBS (pH = 6.1).

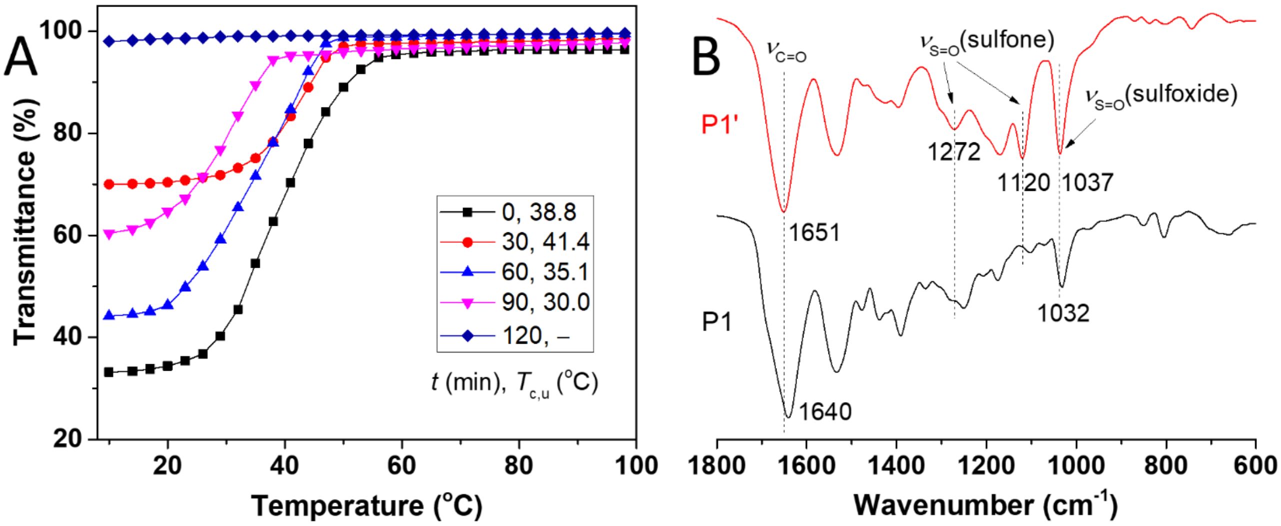

Fig. S15 Temperature-dependent transmittances of polymer aqueous solutions (c_p = 2.0 mg mL^{-1}) obtained by oxidation of P1 solutions for different times (A), and expanded FT-IR spectra of P1 and P1’ (B), in which P1’ is obtained by oxidation of P1 solutions at 25 °C for 24 h.

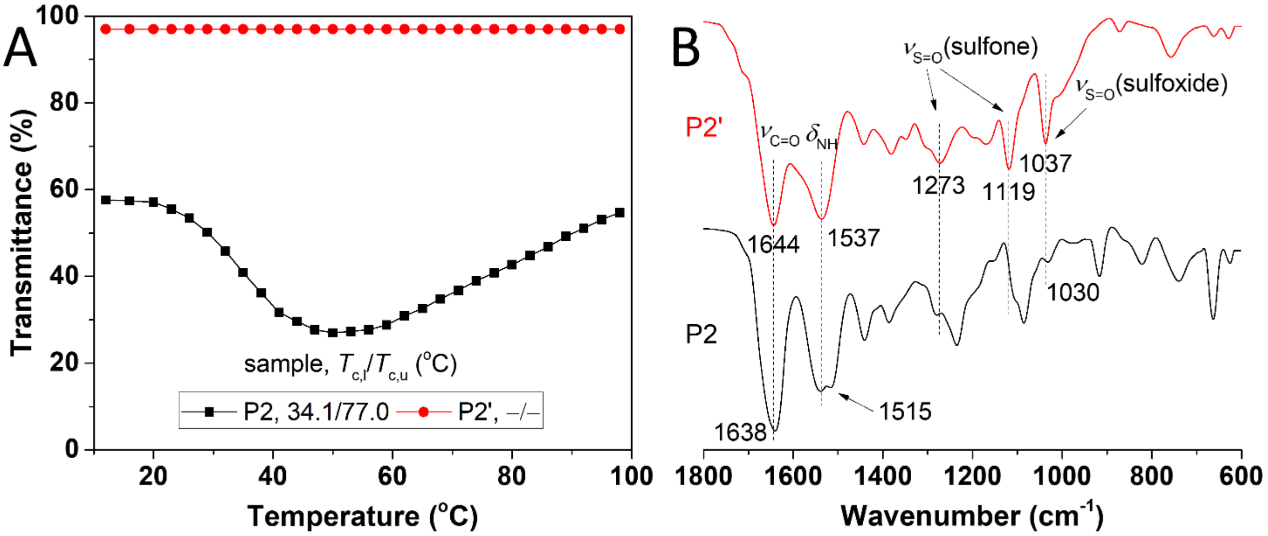

Fig. S16 Temperature-dependent transmittances of polymer aqueous solutions (c_p = 2.0 mg mL^{-1}) formed from P2 and P2’ in PBS (pH = 7.0, A), and expanded FT-IR spectra of P2 and P2’ (B), in which P2’ is obtained by oxidation of P2 solutions at 25 °C for 24 h.

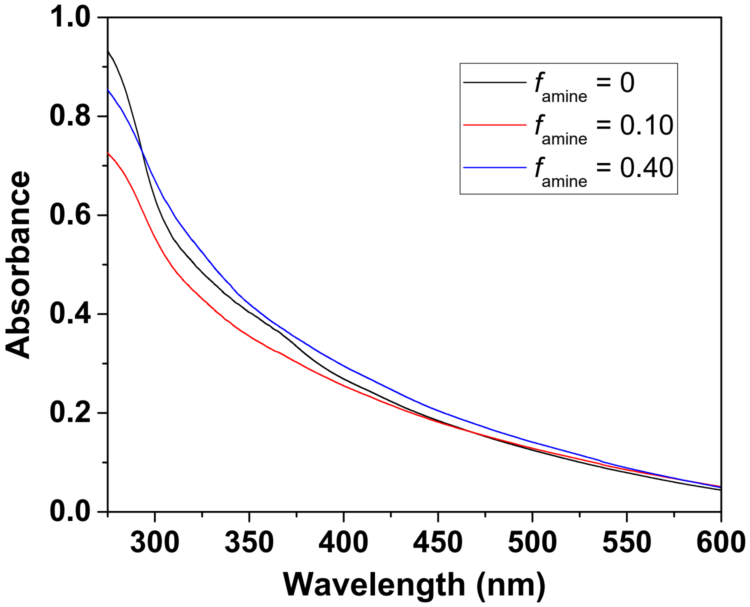

Fig. S17 UV-vis spectra of polymer solutions (c_p = 2.0 mg mL^{-1}) formed from P1 (f_{amine} = 0) and P1/P3 mixture (f_{amine} = 0.10 or 0.40) in PBS (pH = 7.0).

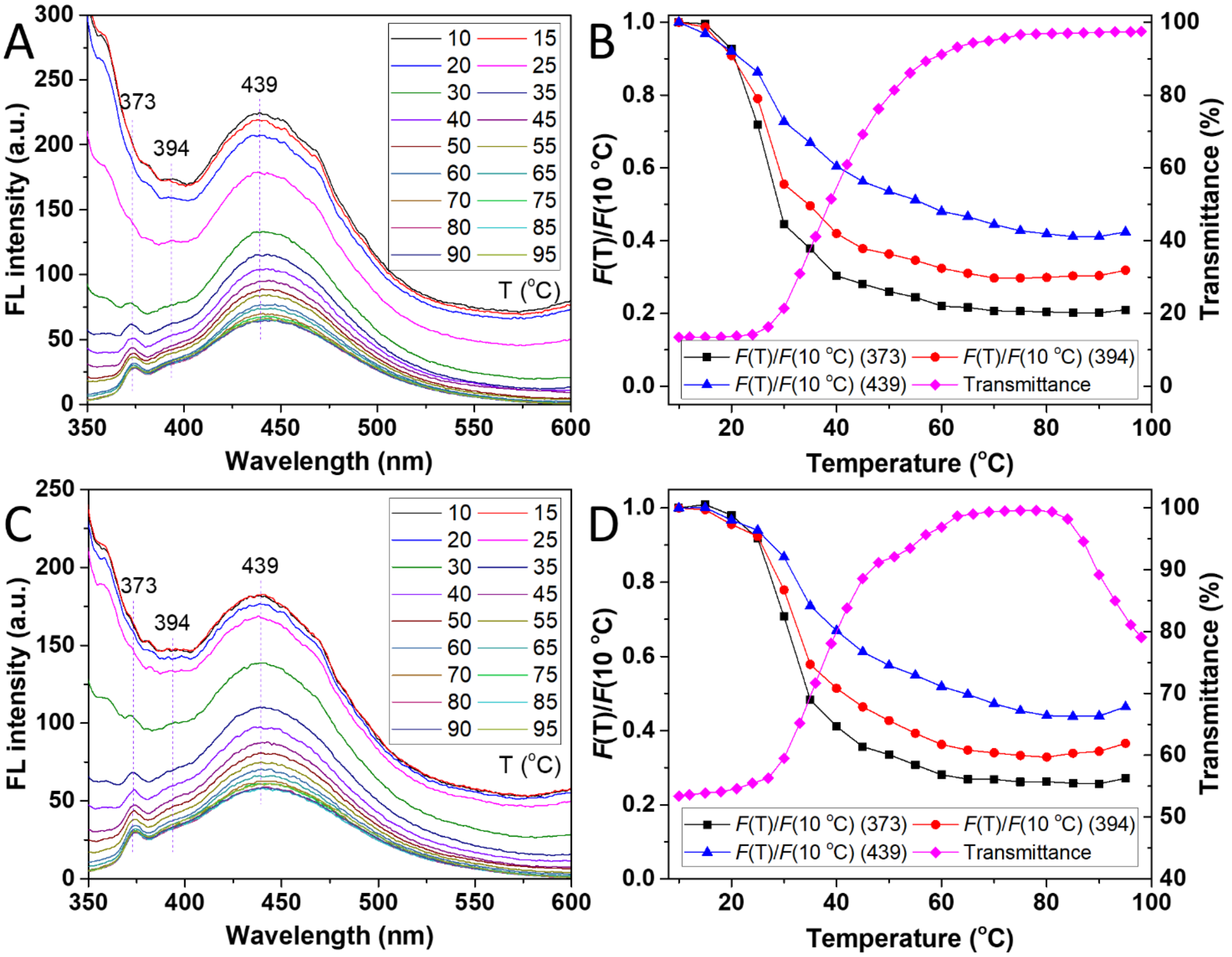

Fig. S18 Temperature-variable fluorescence spectra of polymer solutions ($c_p = 2.0$ mg mL^{-1}, $\lambda_{ex} = 320$ nm) formed P1/P3 mixture ($f_{amine} = 0.10$ (A) and 0.40 (C)) in water during 10 and 95 °C (A, C), and evolution of fluorescence intensity ratio of emission bands at 373, 394 and 439 nm at a fixed temperature (T) and 10 °C (*F*(T)/*F*(10 °C)) and transmittance of polymer solutions ($f_{amine} = 0.10$ (B) and 0.40 (D)) with increasing temperature (B, D), in which *F*(T)/*F*(10 °C) is calculated after baseline calibration.

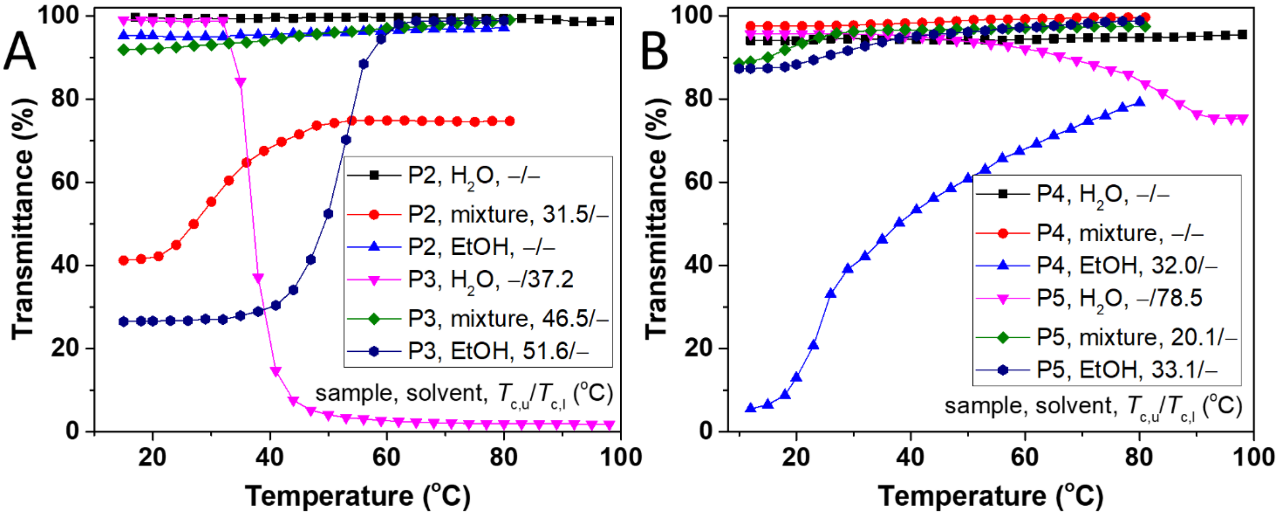

Fig. S19 Temperature-dependent transmittances of polymer solutions ($c_p = 2.0$ mg mL^{-1}) formed from P2/P3 (A) and P4/P5 (B) in water, water/ethanol mixture ($f_{v,\text{ethanol}} = 0.50$) and ethanol.

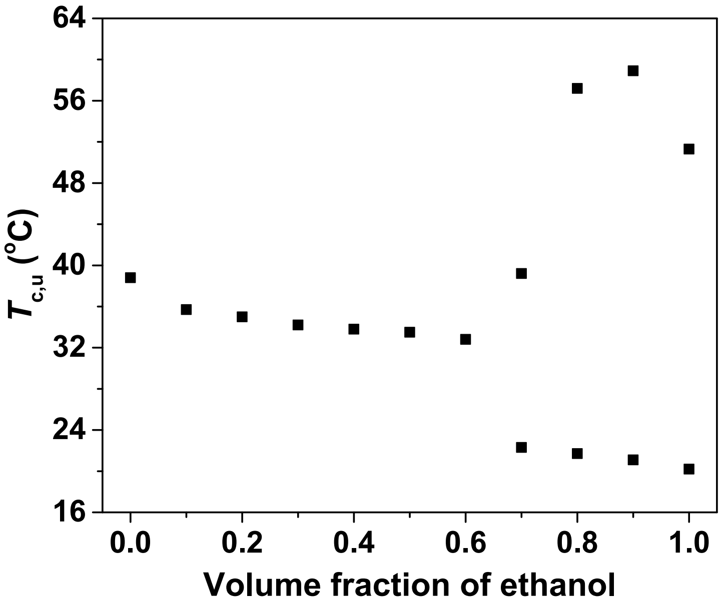

Fig. S20 Dependence of $T_{c,u}$ of P1 solutions (c_p = 2.0 mg mL^{-1}) formed in water, ethanol or their mixture on volume fraction of ethanol.

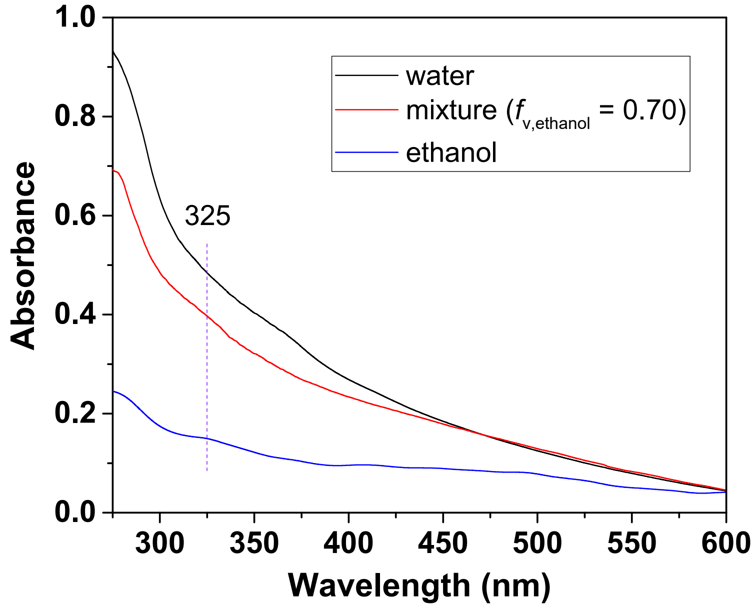

Fig. S21 UV-vis spectra of P1 solutions (c_p = 2.0 mg mL^{-1}) formed in water, ethanol or their mixture ($f_{v,ethanol}$ = 0.70).

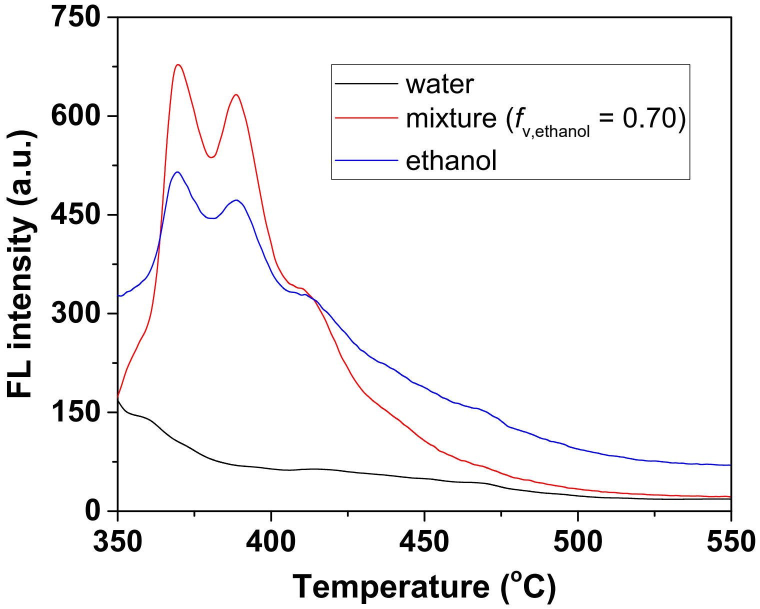

Fig. S22 Fluorescence spectra of P1 solutions (c_p = 2.0 mg mL^{-1}, λ_{ex} = 330 nm) formed in water, ethanol and their mixture ($f_{v,ethanol}$ = 0.70) at 25 °C.

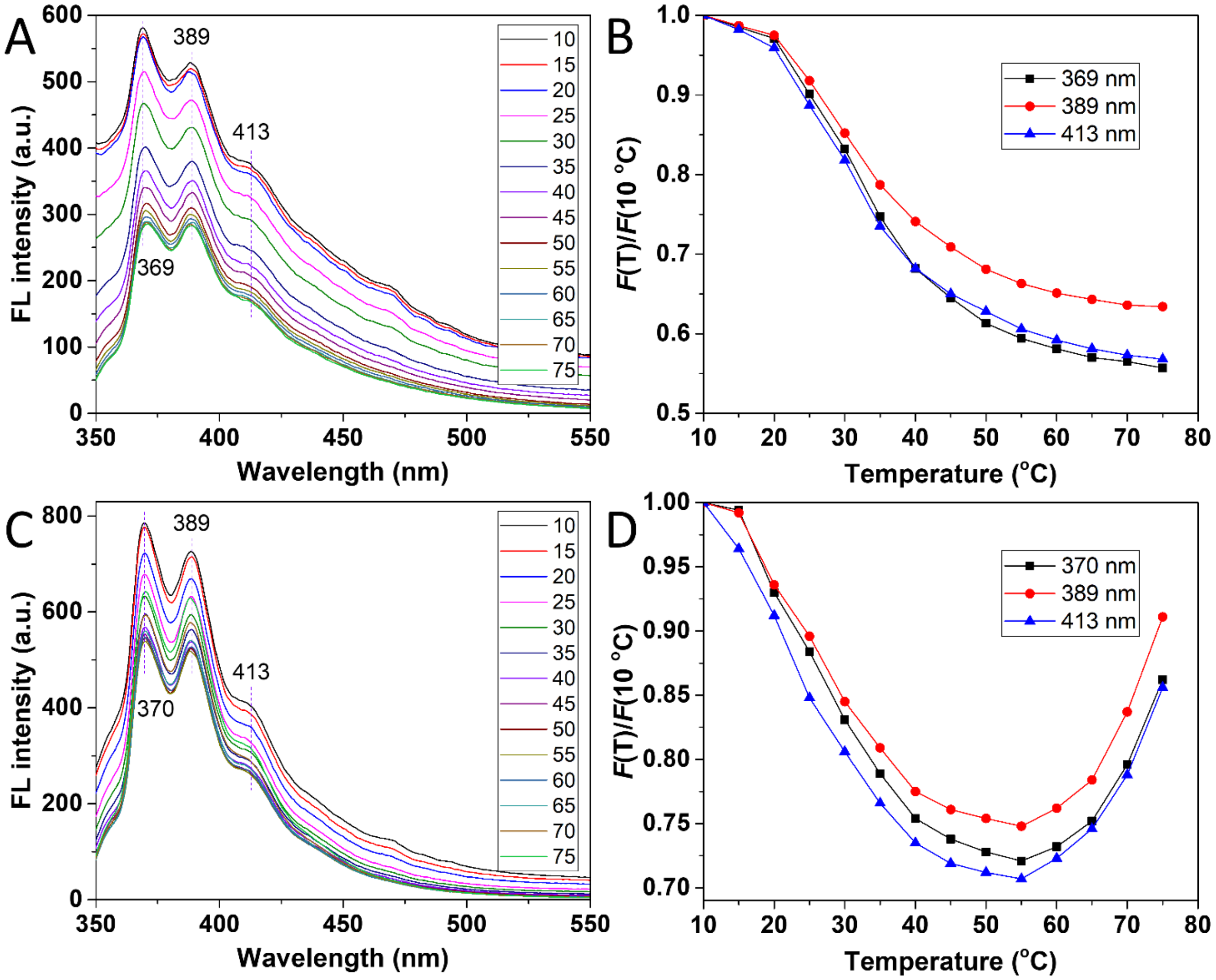

Fig. S23 Temperature-variable fluorescence spectra of P1 solutions (c_p = 2.0 mg mL^{-1}, λ_{ex} = 330 nm) formed in ethanol (A) or water/ethanol mixture ($f_{v,ethanol}$ = 0.70, C) during 10 and 75 °C (A, C), and evolution of fluorescence intensity ratio of emission bands at 369/370, 389 and 413 nm at a fixed temperature (T) and 10 °C (*F*(T)/*F*(10 °C)) with increasing temperature (B, D), in which *F*(T)/*F*(10 °C) is calculated after baseline calibration.

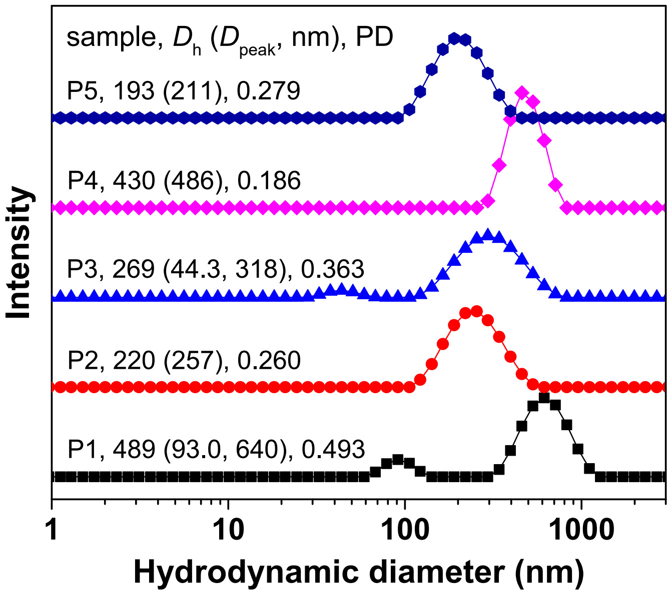

Fig. S24 DLS plots of polymer solutions ($c_p = 2.0$ mg mL^{-1}) formed in water (for P1/P3) and PBS (pH = 6.1 for P2, and 7.0 for P4/P5) at 25 °C.

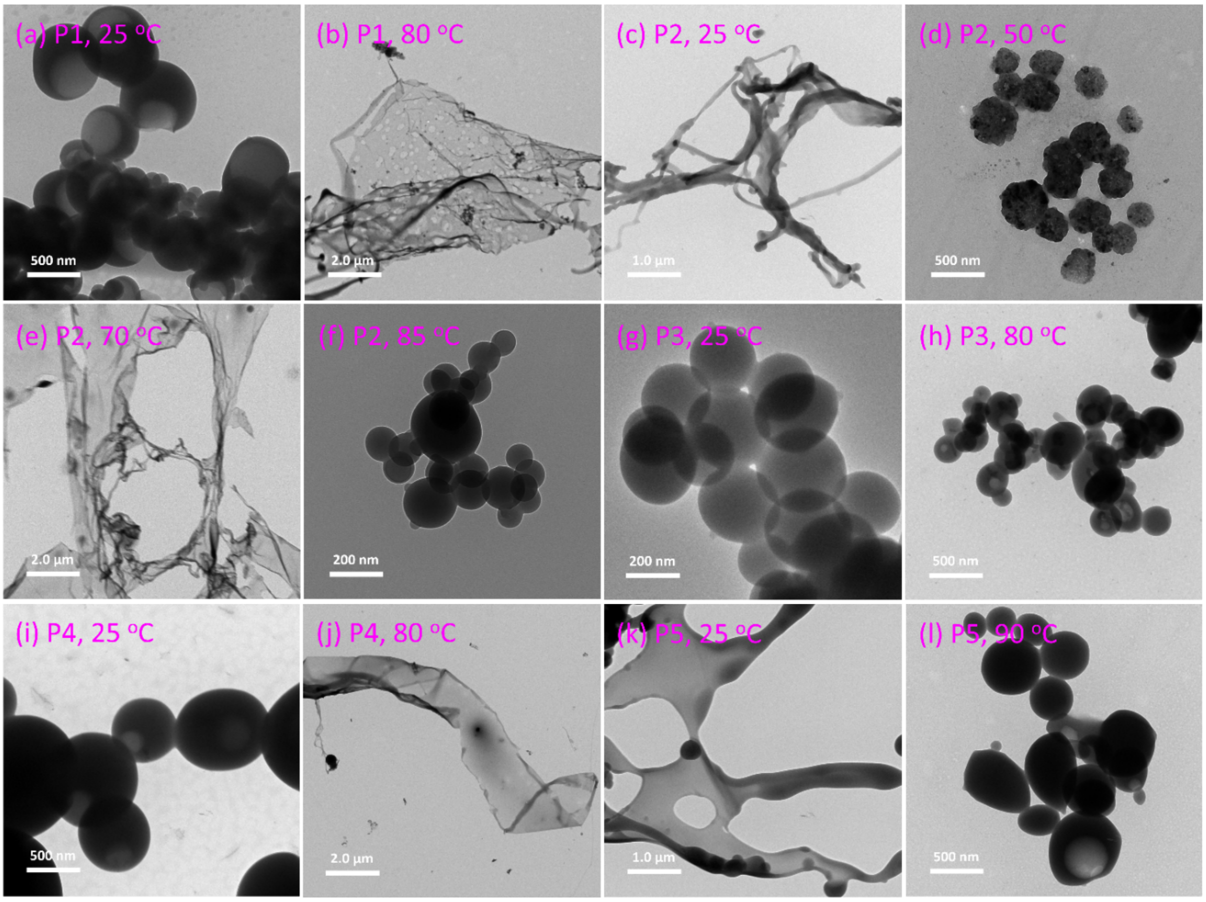

Fig. S25 TEM images of polymer assemblies formed in water (P1: a, b; P3: g, h) or PBS (pH = 6.1 (P2, c-f), and 7.0 (P4: i, j; P5, k, l) at a fixed temperature, and the initial c_p was 2.0 mg mL^{-1}.